Biosensors and Bioelectronics 132 (2019) 310–318

Contents lists available at ScienceDirect

Biosensors and Bioelectronics

journal homepage: www.elsevier.com/locate/bios

# Ultrasensitive detection of hERG potassium channel in single-cell with photocleavable and entropy-driven reactions by using an electrochemical biosensor

Kai Zhang[a,*], Wanting Huang[a], Hao Li[c], Minhao Xie[a], Jiaying Wang[b,*]

[a] Key Laboratory of Nuclear Medicine, Ministry of Health, Jiangsu Key Laboratory of Molecular Nuclear Medicine, Jiangsu Institute of Nuclear Medicine, Wuxi, Jiangsu 214063, China

[b] Department of Rehabilitation & Acupuncture and Moxibustion, Nanjing Medical University, Affiliated Wuxi People's Hospital, Wuxi, Jiangsu 214000, China

[c] School of Biological Science and Technology, University of Jinan, No. 106 Jiwei Road, Jinan, Shandong 250022, China

ARTICLE INFO

*Keywords:*
Ion channel
hERG
Entropy-driven
Exonuclease III
Electrochemical biosensor

ABSTRACT

Ion channel is a pore-forming membrane protein that allows ions to pass through the cell membrane, which is essential for the continuation of life. Analysis of ion channel characteristics at the single cell level will help to study the role of cellular heterogeneity in disease progression and cellular signaling processes. In this study, we fabricate a photocleavable and entropy-driven reaction based electrochemical biosensor for ultrasensitive detection of *human ether-a-go-go related gene* (hERG) potassium channel activity on HEK293 cell. We employed an antibody-DNA1 to conjugate the hERG channel in the cell membrane via antibody-antigen reaction. The release of the DNA1 by photocleavable reaction will trigger an amplification reaction by using the Exonuclease III (Exo III) to generate intermediate DNA. In addition, two hairpin DNA (DNA3 and DNA4) was employed for the signal amplification. We well designed a toehold on DNA3 for intermediate DNA hybridization to form double-strand DNA that opens the DNA3 hairpin. The free DNA3 exposed the relocked toehold domain to open the DNA4. After the entropy-driven toehold-mediated displacement amplification reaction by using intermediate DNA, DNA4 hybridized with DNA3 effectively, making the ferrocene labeled on the 5′-termini DNA4 close to the Au electrode surface to produce the electrochemical response. Then, the displaced intermediate DNA was released from the cell surface into solution for the next entropy-driven reaction. After two steps amplification reaction, one ion channel triggered thousands of DNA3/DNA4 duplex on the biosensor surface. By using this biosensor, electrochemical curve of hERG ion channels on a single cell was obtained.

## 1. Introduction

In single-cell studies, detecting proteins on the surface of cell membranes is becoming increasingly important in clinical diagnosis and biological research (Liu et al., 2016a, 2015). In these proteins, the ion channel is a pore-forming membrane protein that allows ions to pass through the cell membrane, which is essential for the continuation of life and plays an important role in physiological processes. The assay of ion channel in single-cell will help to study the role of cellular heterogeneity in disease progression and cellular signaling processes (Abbas et al., 2011; Shackleton et al., 2009; Tay et al., 2010).

The *human ether-a-go-go related gene* (hERG), which expressed in the nervous tissue and heart, encodes the channel of KV11.1 (a voltage-gated potassium ($K^+$) channel) pore-forming α subunit. In the heart, the hERG plays a very critical role in the repolarization of cardiac action potential, since it constitutes the most rapid component of the delayed rectifier current. Genetic mutations in the hERG give rise to a long QT syndrome associated with chromosome 7 (LQTS type 2), wherein the patient has substantial risk of arrhythmia due to the sudden death, and drug-induced blockade KV11.1 cause QT prolongation. In addition, the hERG potassium channel plays a very important role in regulating tumor cell apoptosis and provides a potential new pathway for the treatment of cancer. Moreover, accurate molecular profiling measurement and analysis of subtype ion channels provides great promise for early disease detection and therapeutic monitoring (Agasti et al., 2012; Issadore et al., 2012). Therefore, the detection method of ion channel in single-cell membrane with high sensitivity and selectivity are in great demand (Altelaar and Heck, 2012; Wu and Singh, 2012). HEK293 cell (human embryonic kidney) line was chosen as a model cell since it is easy to exogenous gene transfection and hERG ion

* Corresponding authors.
*E-mail addresses:* zhangkai@jsinm.org (K. Zhang), wangjiaying@njmu.edu.cn (J. Wang).

https://doi.org/10.1016/j.bios.2019.02.065
Received 18 February 2019; Accepted 26 February 2019
Available online 11 March 2019
0956-5663/ 

channel expression.(Kang et al., 2015; Wang et al., 2016)

However, to date, the work of ion channel determination in cell membranes is rare, and these tasks are mainly dependent on the following two strategies. One is the patch-clamp record model, in which electrophysiological properties of the ion channels can be characterized.(Agasti et al., 2012) The other is using synthesized self-assembling fluorescent probes for the image ion channels we proposed before (Yang et al., 2018). The strategy was based on recognition-driven antibody-ion channels reaction, by newly introducing a platform for amplification. Although these two strategies are important, their use is still limited. These methods need expensive instruments to obtain the patch-clamp data or troublesome fluorophore synthesis for the sensor design, which is unfavorable for potential applications in the clinical assay (Zhou et al., 2018). Hence, it is urgently desirable to develop novel biosensor with easy probe synthesis, and easy ligand modification for the achievement of ultrasensitive assay ion channels in single cell analysis.

In addition, very recently, a lot of DNA-based entropy-driven molecular machines (including DNA walkers, DNA spiders, molecular gears, and tweezers) have been successfully constructed based on the Watson-Crick base pairing rule and duplex melting temperature ($T_m$) difference (Li et al., 2015; Liu et al., 2017; Zhu et al., 2018). Although much effort has been made to develop strategies making use of molecular machines to build biosensing methods, to the best of our knowledge, there is no relevant of using this strategy for building biosensor for ion channel in living cell membrane detection. On the other hand, electrochemical analytical approaches have attracted wide attention due to advantages of easy operation, low cost, fast feedback, etc., and it does not require expensive instruments (Bhuniya et al., 2014; Liu et al., 2016b, 2012; Qian et al., 2015; Sato et al., 2015; Yang et al., 2015; Yu and Wei, 2018; Yuan et al., 2015). Especially in developing ion channel techniques in single cells, electrochemical analysis can be an attractive and promising candidate that is widely used (Fu et al., 2015; Wu and Qu, 2015).

For these reasons, we employed the molecular machines strategy for building an electrochemical biosensor for ion channel assay by employed photocleavable linker molecule as Agasti's report (Agasti et al., 2012). In this method, they employed a photocleavable linker chemical molecule to conjugate specific DNA barcodes and cell membrane proteins' antibodies. The conjugate could target different proteins in cell membrane due to the recognition properties of antibodies via antibody-antigen bridge. The cells were subsequently treated by irradiation, which cleaved the linker, and the DNA barcodes were set free for PCR, and the gel-electrophoresis results can simultaneous identify and quantify multiple proteins on living cells' membranes. Based on the above advantages, we believe that our well-designed electrochemical biosensor could be applied to ion channel determination of live cells by entropy-driven molecular machine's amplification technique, which would enable one-to-multiple amplification after photocleavable reaction.

## 2. Experimental section

### 2.1. Materials

Anti-hERG (rabbit, polyclonal) was obtained from sigma-aldrich (Shanghai, China). The hERG transfected HEK293 cell line was obtained from Cobioer Biotechnology Co. Ltd. (Nanjing, China). The HeLa cell, A549 cell MCF-7 and RPMI-1640 were purchased from KeyGen Biotech. Co. Ltd. (Nanjing, China). 6-mercapto-1-hexanol (MCH), Tris (2-carboxyethyl) phosphine hydrochloride (TCEP), and hexaammineruthenium (III) chloride (RuHex) were purchased from Sigma-Aldrich (St. Louis, MO, U.S.A.). All oligonucleotides used in this strategy were purchased from Genscript Biotechnology Co., Ltd (Nanjing, China) and their sequences were listed in Table 1.

### 2.2. Cell culture

A549 cells, MCF-7 and CCRF-CEM cells were cultured in a flask in Dulbecco's modified Eagle's medium (RPMI-1640, GIBCO), HeLa cells were cultured in a flask in DMEM (GIBCO) supplemented. All media were supplemented with 10% fetal calf serum (FCS, Sigma), penicillin (100 μg $mL^{-1}$), and streptomycin (100 μg $mL^{-1}$) at 37 °C in a humidified atmosphere containing 5% $CO_2$. Cell number was determined with a Petroff-Hausser cell counter (USA). HEK293 cells which stably transfected with hERG $K^+$ channel was cultured with 0.4 mg $mL^{-1}$ zeocin. Cell numbers were determined with a Petroff-Hausser counting chamber (USA) and cell images were obtained on a TCS-SP5 laser scanning confocal microscope (Leica, Germany).

### 2.3. Photocleavable reaction

The antibody-DNA1 was synthesized according previous report (Fig. S1) (Agasti et al., 2012). 100,000 HEK293 cells were incubated with DNA-antibodies (10 μg/mL) in 200 μL PBS solution (pH 7.4, 136 mM NaCl, 2.7 mM KCl, 8.72 mM $Na_2HPO_4$, and 1.41 mM $KH_2PO_4$, 2% FBS and 1% BSA) for 20 min. After centrifugation at 300 g for 3 min and discarding the supernatant solution, HEK293 cells were washed with PBS solution containing (pH 7.4, 136 mM NaCl, 2.7 mM KCl, 8.72 mM $Na_2HPO_4$, and 1.41 mM $KH_2PO_4$ and 2% FBS) for one time and (pH 7.4, 136 mM NaCl, 2.7 mM KCl, 8.72 mM $Na_2HPO_4$, and 1.41 mM $KH_2PO_4$, and 1% BSA) for two times. Then, HEK293 cells were suspended into PBS solution (pH 7.4, 136 mM NaCl, 2.7 mM KCl, 8.72 mM $Na_2HPO_4$, and 1.41 mM $KH_2PO_4$, 0.1% BSA). Then, DNA1-antibody modified HEK293 cells were suspended into PBS solution (pH 7.4, 136 mM NaCl, 2.7 mM KCl, 8.72 mM $Na_2HPO_4$, and 1.41 mM $KH_2PO_4$, 0.1% BSA). Different number of HEK293 cells were then diluted in Eppendorf tubes with different times in 100 μL PBS buffer (pH 7.4, 136 mM NaCl, 2.7 mM KCl, 8.72 mM $Na_2HPO_4$, and 1.41 mM $KH_2PO_4$). Then, diluted cells in PBS buffer solution were exposed at ~365 nm light for 15 min before centrifugation at 300 g for 3 min to separate the DNA1 from the ion channel in the cell surface.

### 2.4. Exo III-aided amplification reactions

For Exo III amplification, (1 μM) DNA2 incubated with DNA1 for 30 min to fabricate the DNA1/DNA2 duplex in 20 μL buffer, then 5 U Exo III were added, and then incubated for another 1 h at 37 °C to produce. After standing for 1 h at 37 °C, the mixtures were incubated at 70 °C for 20 min to deactivate Exo III.

### 2.5. Fabrication of the electrochemical biosensor

A gold electrode was submerged in freshly prepared piranha solution (30% $H_2O_2$: $H_2SO_4$ = 1:3) for 5 min and cleaned thoroughly with dd $H_2O$ afterwards. Then, the gold electrode was carefully polished with sand papers and mirror surface alumina slurry (1.0, 0.3, and 0.05 μm diameter each) and subsequently sonicated successively in ethanol and water for 5 min. Finally, the electrode was electrochemically cleaned in 0.5 M $H_2SO_4$ by scanning the potential from −0.2 to +1.6 V until a stable cyclic voltammogram was obtained. The electrode was then thoroughly washed with ultrapure water and dried under purified nitrogen.

Upon denaturation at 95 °C for 5 min and subsequent renaturation by slowly cooling to room temperature for about 4 h, the DNA3 forms a hairpin structure effectively. Then, TCEP (1 mM) was added to DNA3 solution for 1 h to reduce disulfide bonds, following a dilution with Tris-HCl buffer (50 mM, pH 7.4, 10 mM KCl, 5 mM $MgCl_2$, and 0.1 M NaCl) to get 0.3 μM DNA3. Then 6 μL of DNA3 (0.3 μM) was dropped on the cleaned gold electrode surface and incubated at 4 °C for 12 h to form a self-assembled monolayer of DNA3. After washing with 10 mM PBS (pH 7.4, 0.1 M NaCl) and drying with flowing nitrogen, 6 μL of MCH in an

**Table 1**
The sequences used in this strategy.

| Note | Sequence (5′-3′) |
|---|---|
| DNA1 | HS-AAGGCAGGAAGACAAACA |
| DNA1-cy3 | HS-AAGGCAGGAAGACAAACA-cy3 |
| DNA1a | HS-AAGGTAGGAAAACAAACA |
| DNA1b | HS-AAGGCAGTAATACAAACA |
| DNA1c | HS-AAGGCAAGAAGATAAACA |
| DNA2 | CGACATCTAACCTAGCGCTAGCTCATGAGCTAGCGCTAGGTTAGATGTCGTGTTTGTCTTCCTGCC |
| Intermediate DNA | CGACATCTAACCTAGCGCTAGCTCA |
| DNA3 | HS-GTCAGTGAGCTAGCGCTAGGTTAGATGTCGCCATGTGTAGACGACATCTAACCTAGC |
| DNA4 | AGATGTCGTCTACACATGGCGACATCTAACCTAGCCCATGTGTAGA-Fc |
| DNA5 | SH-TTATGTGACTGTTTGTCTTCCTGCCTTGTCACAT-Fc |
| DNA6 | HS-GTCAGTGTTTGTCTTCCTGCCTTCCATGTGTAGAAAGGCAGGAAGACAA |
| DNA7 | CCTGCCTTTCTACACATGGAAGGCAGTGTGTAGAAA-Fc |

aqueous solution (1 mM) was dropped on the electrode surface for 1 h to fill the pinholes in the DNA3 monolayer. After washing with PBS and drying with purified nitrogen, the biosensor was obtained and stored at 4 °C for further use.

### 2.6. Measurement procedure

First, the intermediate DNA and DNA4 (1 μM) in Tris-HCl buffer (50 mM, pH 7.4, 10 mM KCl, 5 mM $MgCl_2$, and 0.1 M NaCl) was mixed incubated at room temperature for 10 min 6 μL of the mixture solution was dropped on the biosensor surface for 60 min at room temperature to achieve the entropy-driven amplification reaction. After washing with 10 mM PBS (pH 7.4), the electrochemical biosensor was immersed in 10 mM PBS (pH 7.4, 136 mM NaCl, 2.7 mM KCl, 8.72 mM $Na_2HPO_4$, and 1.41 mM $KH_2PO_4$, and 0.1 M $NaClO_4$) for alternating current voltammetric (ACV) assays and in 10 mM Tris-HCl buffer containing 50 μM RuHex for Chronocoulometric (CC) measurements on CHI 660E electrochemical workstation (CH Instruments)(a Pt wire as counter electrode, a Ag/AgCl electrode as reference electrode, and an Au electrode with 2 mm diameter as working electrode). For ACV assays, scan from 0 to +0.6 V with a 4-mV step potential and the frequency and amplitude are 25 Hz and 0.025 V, respectively. For CC measurements, two-step potential was used with 250 ms duration scan from 500 mV to 0 mV in 10 mM Tris-HCl buffer (pH 7.4, 50 μM RuHex).

## 3. Results and discussion

### 3.1. The working principle

We fabricate a photocleavable and entropy-driven reaction based electrochemical biosensor for ultrasensitive detection of hERG potassium channel activity on HEK293 cell. The application of photocleavable linker makes itself became an effective tool which changed cell membrane protein to free DNA. The synthesis process of the Antibody-DNA was indicated in the Scheme S1 and the ion channel ultrasensitive assay strategy is shown in Scheme 1. The antibody-DNA1 conjugated with the hERG channel in the cell membrane via antibody-antigen reaction. Then the Antibody-DNA conjugate living cell exposed in light for 15 min to release the DNA (DNA1 in Scheme 1) for next amplification steps by using Exonuclease III (Exo III). The DNA2 forms a duplex with 3′ protruding termini to ensure itself cannot be digested by Exo III since Exo III only digests dsDNA strands with blunt or 3′-recessed termini (Cui et al., 2011; Zhou et al., 2013). The hybridization of DNA1/DNA2 (form DNA1/DNA2 duplex) makes the DNA2 has a 3′-recessed termini for Exo III digestion. The Exo III assisted DNA2-cleavage cycle to release DNA1 for next digestion reaction and intermediate DNA for entropy-driven reaction on the Au electrode surface. Two hairpin DNA (DNA3 and DNA4) was employed for the signal amplification. The formation of locked DNA3 hairpin structure, which modified on the electrode surface, makes DNA4 not hybridize with itself effectively. A toehold on DNA3 was designed for intermediate DNA hybridizaing in order to open the DNA3 hairpin. The free DNA3 exposed the relocked toehold domain to open the DNA4. After the entropy-driven toehold-mediated displacement amplification reaction, DNA4 hybridized with DNA3 effectively, making the ferrocene (Fc) labeled on the 5′-termini DNA4 close to the Au electrode surface to produce the electrochemical response. Then, the displaced intermediate DNA was released from the cell surface into solution for the next entropy-driven reaction. After two steps amplification reaction, one ion channel triggered thousands of DNA3/DNA4 duplex on the biosensor surface. So, the ACV signal of the biosensor can be used for quantitation of ion channel in cell membrane.

### 3.2. Optimization of experimental conditions

The density of DNA3 on the Au electrode was a key experimental parameter to the entropy-driven reaction. Both low and high density was unconducive to the formation of DNA3/intermediate DNA duplex, since the low DNA3 density conducive to the hybridization of intermediate DNA to DNA3, since the low concentration of DNA3 abolished the distance-dependent DNA3/intermediate DNA hybridization reaction, and the high density composed steric hindrance to constrain the toehold-based hairpin open reaction. Thus, the density of DNA3 modified on the biosensor was optimized by changing the incubated concentration of DNA3. From Fig. 1A, we obtained that 0.3 μM given the highest ACV response. So, we chose 0.3 μM DNA3 for the biosensor fabrication. Also, to get the highest response, 1 μM DNA4 was obtained for the entropy-driven amplification reaction (Fig. 1B).

Then, the immobilized DNA3 density on the electrochemical biosensor surface was calculated via the Cottrell formula and Faraday's equation by using Chronocoulometry measurements (ruthenium (III) hexaammine (RuHex) was employed as a redox molecules) (Lin et al., 2016; Steel et al., 1998; Yang et al., 2016; Yao et al., 2014).

$$Q_d = 2nFAC^*\left(\frac{Dt}{\pi}\right)^{1/2} + Q_{dl} + Q_{ads}$$

$$Q_{ads} = nFA\Gamma_0$$

$$\Gamma_{DNA} = \Gamma_0\left(\frac{z}{m}\right)(N_A)$$

The meaning of symbols in the formulas are list in Table 2.

An Anson plot of Qd versus $t^{1/2}$ was plotted to display the CC data (Fig. 1C). The $Q_{dl} + Q_{ads}$ value was corresponded at the intercept of t = 0 ($Q_d$ value) in the presence of saturated $Ru(NH_3)_6^{3+}$ solution. In the absence of $Ru(NH_3)_6^{3+}$, Q = $Q_{dl}$ at the intercept of t = 0. Once $Q_{dl}$ is obtained, Γ0 can be calculated in the presence of saturated $Ru(NH_3)_6^{3+}$ solution. The density of DNA3 on the Au electrode surface was calculated about $3.5 \times 10^{12}$ molecules/$cm^2$ from the surface excess of RuHex. The average intermolecular distance was calculated by using the follow equation:

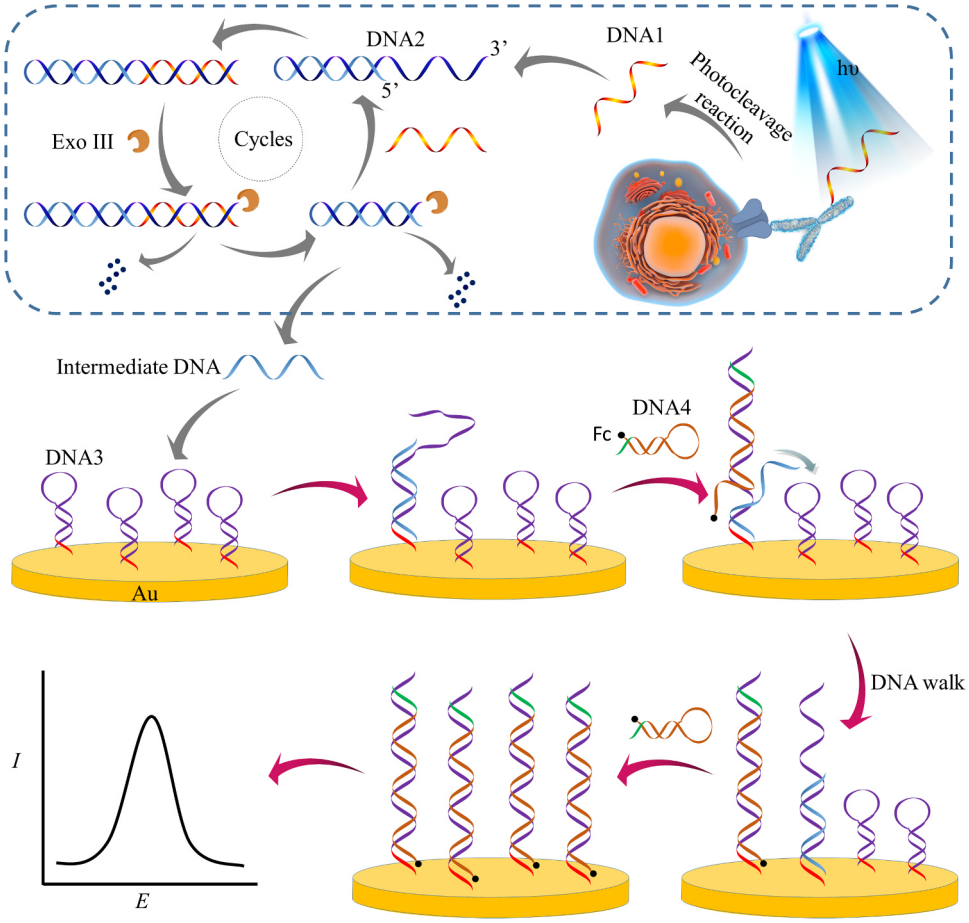


**Scheme 1.** Schematic illustration of the photocleavable cleavage and entropy-driven amplification-based biosensor for the assay ion channel in single-cell cell membrane.

$$d = \left(\frac{A}{\Gamma_{DNA}}\right)^{1/2}$$

where d is the intermolecular distance of DNA3 and A is the unit area (1 $cm^2$). The distance calculated about 5.3 nm.

This intermolecular distance of DNA3 was long enough to reduce the steric hindrance to intermediate DNA since the length of intermediate DNA is 8.5 nm (25 bp, given 0.34 nm per bp) between DNA3, which may influence the hybridization of interaction between intermediate DNA and DNA4 and the formation of DNA3/DNA4 duplex. And the length of intermediate DNA is longer than the intermolecular distance of modified DNA3, so this length can give the best performance of the amplification reaction on the electrode surface (Yao et al., 2014). The stability of the prepared biosensor was analysied by using different stored times. Fig. S2 indicated that the biosensor was exhibited high stability even stored for 48 h.

The time of the entropy-driven amplification reaction was then investigated. As shown in Fig. 1D, the ACV signals (1000 cells (a) and 10,000 cells (b)) increased with the incubation time and reached the plateaus after about 60 min incubation. Therefore, an incubation time of 60 min was chosen for the next molecular machines reaction.

### *3.3. Characterization and feasibility of the photocleavable reaction and entropy-driven amplification reaction strategy*

Electrochemical Impedance Spectroscope (EIS) measurements were performed in 5 mM $K_3[Fe(CN)_6]/K_4[Fe(CN)_6]$ (1:1) to characterize step by step reactions by using our electrochemical biosensor (Fig. 2A). The bare electrode showed an elatively small electronic charge transfer resistance ($R_{ct}$) (Fig. 2A, curve a) due to its fast charge-transfer process. After the modification of DNA3 and MCH, $R_{ct}$ greatly increased (Fig. 2A, curve b) because the negative-charged phosphate skeletons of the DNA3 monolayer and MCH monolayer repelled $[Fe(CN)_6]^{3-/4-}$ from the electrode surface, suggesting the successful preparation of the electrochemical biosensor. The $R_{ct}$ slightly changed after the biosensor was incubated with the DNA4, indicating the DNA4 could not hybridize directly with DNA3 (Fig. 2A, curve c). When the biosensor treated with intermediate DNA, a larger $R_{ct}$ was obtained (Fig. 2A, curve d), indicating the intermediate DNA may hybridize directly with DNA3. However, since the low amount of intermediate DNA, few intermediate DNA/DNA3 duplex formed on the electrode. In the presence of intermediate DNA and DNA4, $R_{ct}$ was enhanced greatly (Fig. 2A, curve e) due to the formation of DNA3/DNA4 duplex, which triggered by the intermediate DNA through DNA walker amplification reaction.

The feasibility of the photocleavable reaction and entropy-driven amplification reaction for ion channels in cell membrane assay was verified by determining the biosensor' ACV response by treated with or without HEK293 cells (Fig. 2B, curve a to d). It can be observed from the data that the high ACV curve depends on the present of HEK293 cell and DNA4, demonstrating that the ACV signal is ascribed to the photocleavable reaction and molecular machines' amplification technique. When the sensing platform is directly treated with living cells and DNA4, the amplification reaction results in a large ACV response (curve c and d). Otherwise, when HEK293 cell is absence in the system, fewer intermediate DNA generated for the amplification reaction, so a lower amount of DNA4 is loaded onto the biosensor surface which leads to a tiny ACV response can be obtained (curve b). Therefore, the ion channel in the cell membranes, which can be reflected by the photocleavage

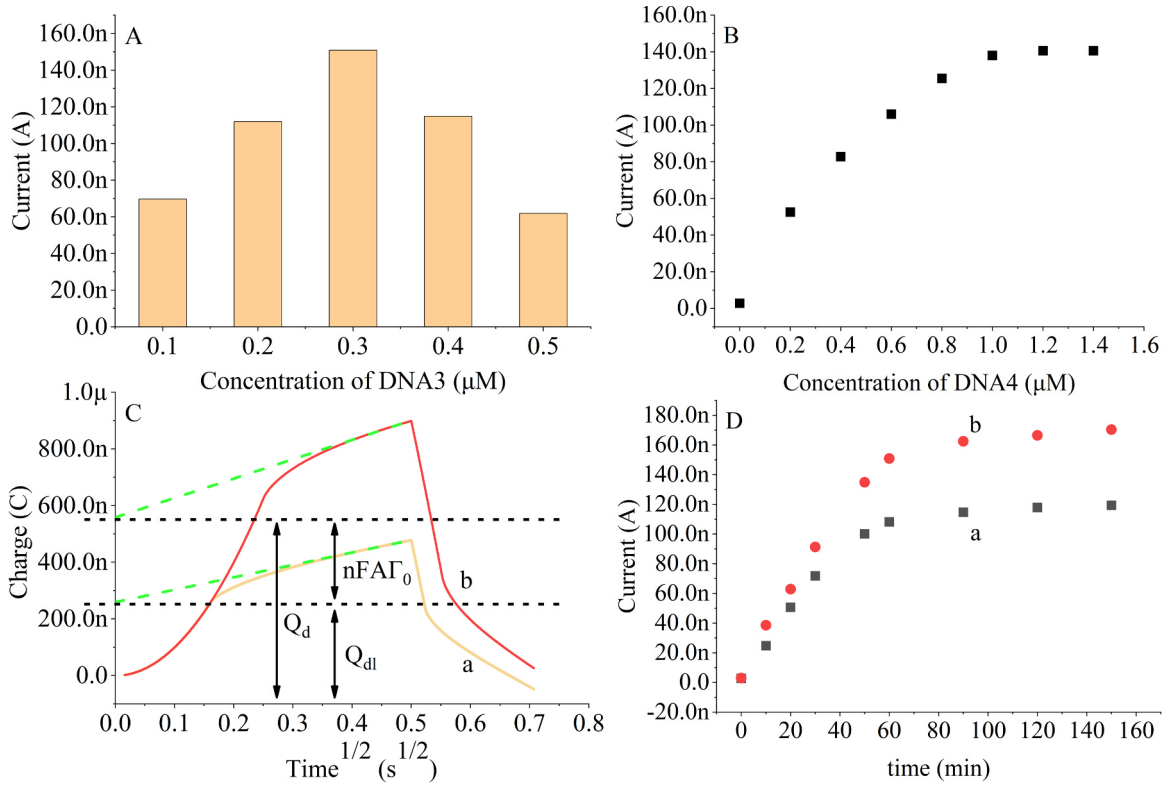


**Fig. 1.** (A) Concentration of DNA3 optimization. (B) Concentration of DNA4 optimization. (C) Chronocoulometric curves of (a) MCH modified electrode and (b) and DNA3 modified electrode. All data obtained in 10 μM Tris-HCl buffer containing 50 μM RuHex. (D) Entropy-driven amplification time by treated with (a) 1000 and (b) 10,000 counts HEK293 cell.

**Table 2**
The meaning of the symbols in the formulas.

| Name | Meaning | Note |
|---|---|---|
| $Q_d$ | Charge | |
| F | Faraday constant | 96 485 C/mol |
| n | Electrons number per molecule for reduction | n = 1 |
| *A* | Work electrode area | 0.0314 $cm^2$ |
| $C^*$ | RuHex bulk concentration | mol $cm^{-3}$ |
| *D* | Diffusion coefficient | $cm^2$ $s^{-1}$ |
| *t* | Reaction time | s |
| $Q_{dl}$ | Capacitive charge | C, coulomb |
| Qads | Charge produced by RuHex | |
| $\Gamma_0$ | Quantity of the adsorbed reactant ($Ru(NH_3)_6^{3+}$) | mol $cm^{-2}$ |
| $\Gamma_{DNA}$ | DNA3 density | molecules $cm^{-2}$ |
| *m* | The number of DNA3 bases | 51 bases |
| *z* | Charge of the redox molecule (RuHex) | For RuHex, z is 3 |
| $N_A$ | Avogadro's number | $6.02 \times 10^{23}$ $mol^{-1}$ |

reaction and entropy-driven reaction, correlates with the electrochemical signal intensity of the biosensor.

### 3.4. Efficiency of two amplification steps

To demonstrate the efficiency of two amplification steps, two experiments were designed and performed. For the first control experiment, photocleavable reaction generated DNA1 directly detected by an electrochemical biosensor. The biosensor was fabricate an Fc modified hairpin DNA (DNA5) on Au electrode surface (Scheme 2A). By using this biosensor, 10,000 counts cell can trigger an observable ACV signal reduction (Fig. 3A and B). This biosensor has a poor sensitivity for the ion channel assay in cell.

The second control experiment is performed by a biosensor which employed a hairpin DNA (DNA6) modifying on the Au electrode (Scheme 2B). Fc modified hairpin DNA (DNA7) was also employed to generate the ACV signal. In this system, DNA1 and DNA7 treating the DNA6 modified Au electrode may trigger the entropy-driven toehold-mediated displacement amplification reaction. The reaction also makes the Fc close to the Au electrode surface to produce an ACV response. By using this biosensor, even 100 counts cell can trigger an ACV signal (Fig. 3C and D), this biosensor also exhibit a poor sensitivity for the ion channel assay in single cell.

### 3.5. Assay performance

In order to test the response of the method to HEK293 cells, the electrochemical signal of the DNA4 was recorded at different incubation concentrations of HEK293 cells, which performed dilution experiments. Fig. 4A shows the ACV signal following two stages amplification reactions from different numbers of cells. A significant increase in the ACV signal was observed with the increasing HEK293 cell concentrations from 1 to 10,000 cells. A Petroff-Hausser cell counter consisted of 25 groups of 16 small squares was utilized to count the amount of the total cell. One drop of cell suspension was pipetted into the middle of the counting plate covered with a coverslip. The cell suspension fills the counting chamber without generating bubbles while the excess suspension is sucked up with absorbent paper. Then the cell counter was placed under a microscope after the cell had been distributed well in the counting chamber. As for performing the counting, the cells in five large squares of the upper left, lower left, upper right, lower right, and middle square is counted according to the diagonal orientation. Furthermore, the statistics of the cells that settle on the grid line are stipulated, that only the cells on two adjacent lines are counted to ensure the accuracy of counting. Afterward, different number cells solutions were prepared by dilution.

For single-cell assay, to ensure that the tube contains a single-cell, the cell was imaged to find by using TCS-SP5 laser scanning confocal microscope. After that, the single-cell was transferred to a tube in PBS

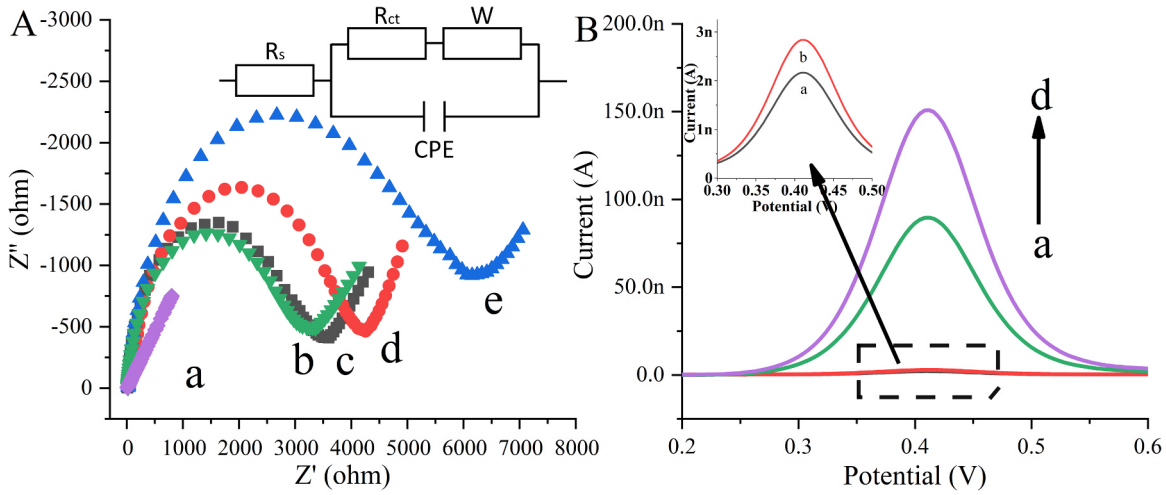


**Fig. 2.** (A) Electrochemical impedance Spectroscope (EIS) for the electrode with different modified layers in 5 mM $K_3Fe(CN)_6$ and $K_4Fe(CN)_6$: (a) bare electrode, (b) the biosensor (DNA3 (0.3 μM) and MCH modified electrode,) (c) the biosensor treated with DNA4 (1 μM), (d) the biosensor treated with intermediate DNA (10,000 cell), and (e) the biosensor treated with intermediate DNA and DNA4. Inset is the equivalent circuit applied to fit to the measured data and consists of the ohmic resistance ($R_s$) of the electrolyte solution, the electronic charge transfer resistance ($R_{ct}$), in series with the finite length Warburg (W), and in parallel with a constant phase element (CPE). (B) Feasibility assay with different conditions. (a) the ACV curve of the biosensor (2.17 ± 1.02 nA, average value ± standard deviation) (modified with MCH); (b) the ACV curve of the biosensor treated with DNA4 (2.84 ± 1.28 nA); the ACV curves of the biosensor treated with DNA4 and HEK293 cells (10,000 counts) for 20 min (89.7 ± 5.82 nM) (c) and 60 min (150.9 ± 6.28 nA) (d). The insert indicates the curve a and b.

buffer for the next experiments. Fig. 4A insert images showing a single HEK293 cell imaged by microscope for original magnification 200× (20× objective lens, 10× ocular lens). Analysis of ion channels in a single HEK293 cell using the biosensor was also proposed. Following the two steps amplification, an ACV curve recorded from the tubes containing single HEK293 cell produced a relative high ACV curve (curve b, 6.07 ± 1.32 nA) towards the background (curve a, 2.84 ± 1.28 nA). This result indicates that the electrochemical biosensor provides analysis of hERG ion channels on a single cell. The ultrahigh sensitivity of the biosensor is from the one-to-multiple isothermal amplification manner of Exo III and highly effective of entropy-driven molecular machines amplification technique, resulting in an amplification electrochemical signal even if the amount of target ion channels on single-cell. The high sensitivity may attribute the success to the antibody-antigen reaction in the cell surface. The reaction is verified by using fluorophore (cy3) modified DNA1 (DNA1-cy3, Table 1). After incubated with DNA1-cy3 modified antibody, the cell shows bright fluorescence (Fig. S3), which indicated the successful reaction of antibody and ion channel.

Fig. 4B illustrates the ACV signal in responding to the different HEK293 cell concentrations. About 10-fold curve is clearly observed at the concentration of 80 compared (curve g) with 1 count cell (curve b). The ACV signal value is linearly dependent on the logarithm of HEK293 cell concentration in the ranges 1–10000 counts, with a correlation equation of $Y = 1.66 \times 10^{-9} + 3.56 \times 10^{-8}$ lgX ($R^2 = 0.9852$), where Y is the ACV curve signal and X is the concentration of HEK293 cell. The detection limit of our biosensor was calculated as one count cell based on 3σ method (blank plus 3× standard deviations). In addition, by using this biosensor, the ACV response signal of a single-cell can obtained (Fig. 4A, line b). A linear range from 0 to 10 cells using an equation $Y = 3.77 \times 10^{-9} + 3.64 \times 10^{-9}$ X ($R^2 = 0.9706$) (Fig. 4B insert), where Y is the ACV curve signal and X is the concentration of HEK293 cell. The slop of the linear equation ($\Delta I$ per cell) indicate the biosensor sensitivity (Elsholz et al., 2009). Since one cell can trigger $3.64 \times 10^{-9}$ nA ACV response, our biosensor is sensitive enough to assay single-cell.

### 3.6. Specificity assay

The specificity of the photocleavable and entropy-driven reactions-based biosensor for ion channel assay was evaluated with two control experiments: (a) the sequences contain mutant bases in DNA1 and (b) four irrelevant cell lines (HeLa, A549, MCF-7 and CCRF-CEM, random selection) which not express hERG ion channel in the cell membranes. Three DNA sequences (DNA1a, DNA2b, and DNA3) that possessed the mutant bases in DNA1 had been employed (Table 1). Equal

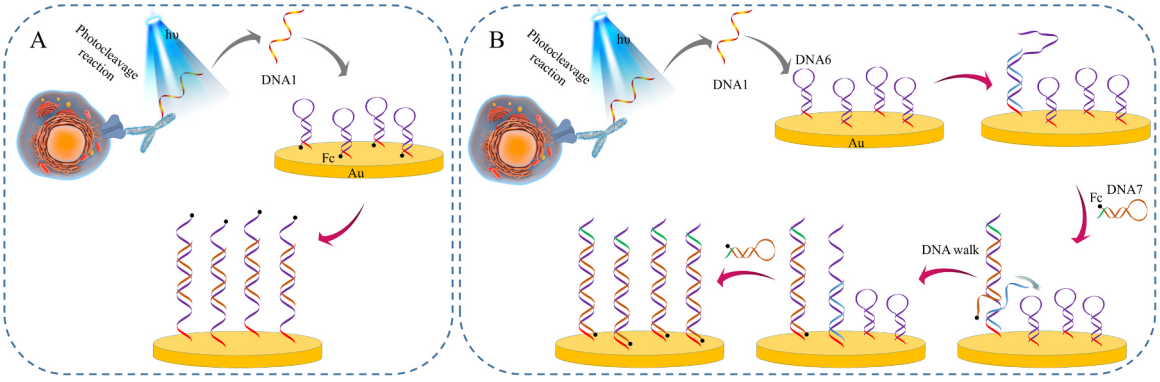


**Scheme 2.** Schematic illustration of biosensor for other two control experiments for the assay ion channel in single-cell cell membrane. (A) Direct detected by using a biosensor and without amplification method and (B) entropy-driven amplification-based biosensor for the assay.

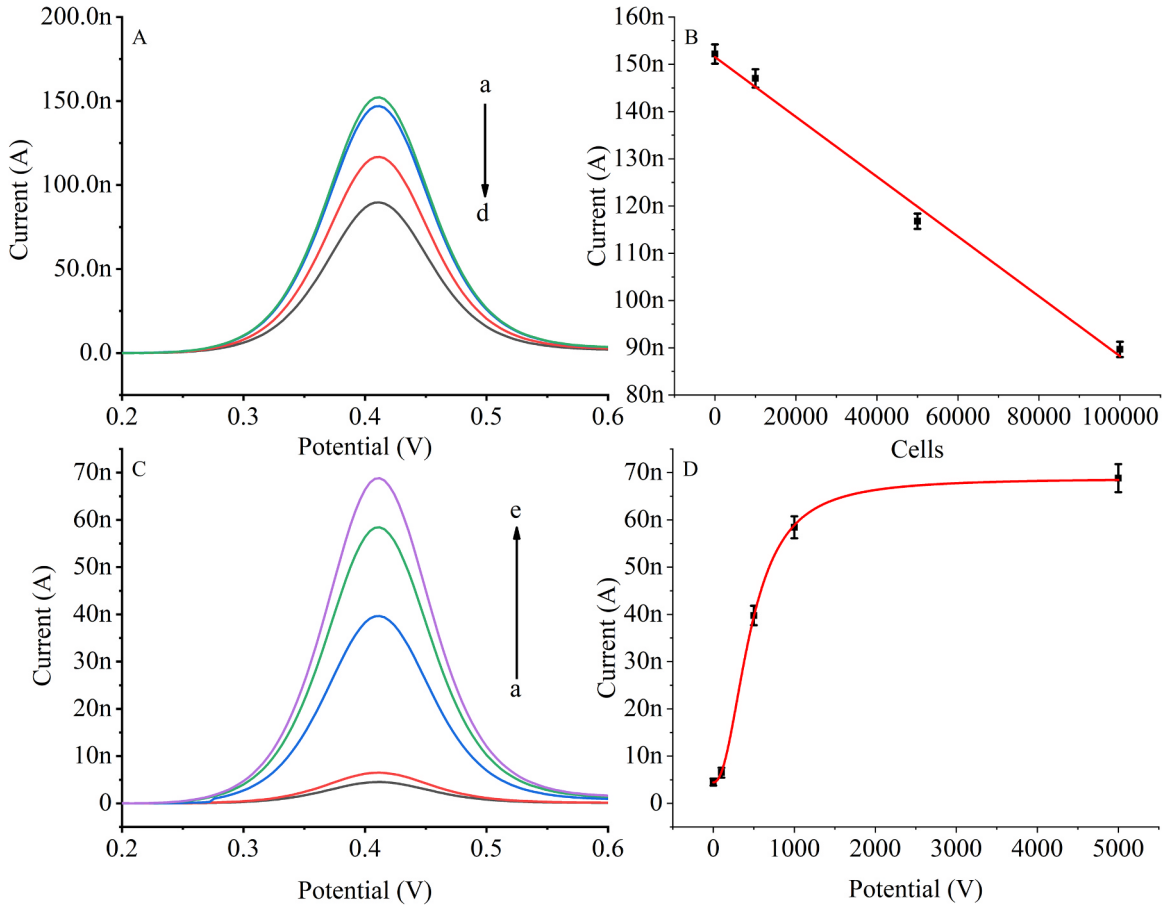


**Fig. 3.** Detection sensitivity of the biosensors. (A) ACV curve of the biosensor show in Scheme 2A for the assay of ion channel in HEK293 cells at different concentrations (0, 10,000, 50,000 and 100,000 from a to d). (B) The relationship between the ACV curve and the concentrations of HEK293 cells. (C) ACV curve of the biosensor show in Scheme 2A for the assay of ion channel in HEK293 cells at different concentrations (0, 100, 500, 1000 and 5000 from a to e). All the data are taken from independent experiments with repetition for at least three times, and the presented data are the results of averaging.

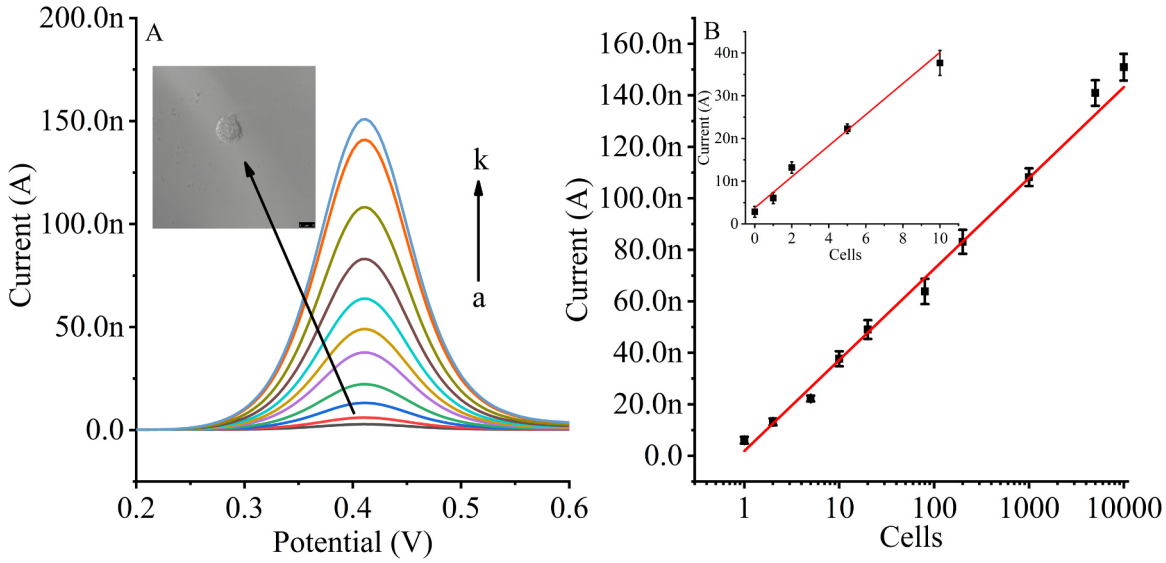


**Fig. 4.** Detection sensitivity of the biosensor. (a) ACV curve of the strategy for the assay of ion channel in HEK293 cells at different concentrations (0, 1, 2, 5, 10, 20, 80, 200, 1000, 5000, and 10,000 from a to k). Image showing a single HEK293 cell (Scar bar: 10 μm). (B) The relationship between the ACV curve and the logarithm concentrations of HEK293 cells. Insert shows a linear relationship over the range from 0 to 10 counts cells. All the data are taken from independent experiments with repetition for at least three times, and the presented data are the results of averaging.

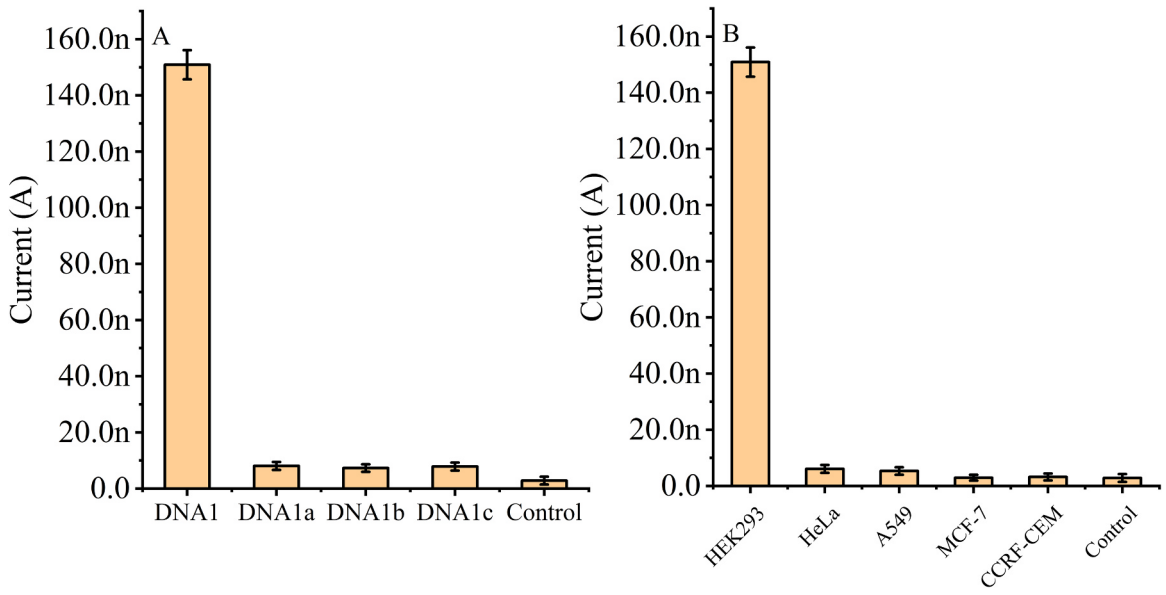


**Fig. 5.** Specificity assay of the method. (A) Comparing the ACV signals from HEK293 cells by treated with antibody-DNA1, antibody-DNA1a, antibody-DNA1b, and antibody-DNA1c. (B) Comparing the ACV signals from HEK293 and other cell lines (HeLa, A549, MCF-7 and CCRF-CEM). Concentrations of the cells are all 10,000. All the data are taken from independent experiments with repetition for at least three times, and the presented data are the results of averaging.

concentrations of DNA1/DNA2 duplex and control sequences (DNA1a, DNA1b, and DNA1c)/DNA2 duplexes were incubated with 10,000 HEK293 cells. After two steps amplification, there was no obvious ACV signal obtained in the presence of control sequences (Fig. 5A). The capability for mismatch discrimination was resulting from the DNA1 and DNA2 hybridization step, which was highly dominated by the Exo III well digest capability that discriminate perfect and non-perfect matched duplexes efficiently.

A major challenge for ion channel investigation in cell membranes is the capability to discriminate other cell lines, which is greatly important for a better understanding of the preclinical diagnostics and pathogenic mechanism of single-cell. Therefore, the specificity of the proposed biosensor was investigated in the presence of other control cell lines, which showed no expression of the hERG ion channels. Control cells produced an electrochemical signal only somewhat larger than the control experiment (in the absence of HEK293 cell), which were distinctly lower than that for HEK293 cells (Fig. 5B). This high selectivity was derived from the capacity of the recognition of the antibody with ion channel. These results indicted the high specificity of the proposed photocleavable and entropy-driven reactions-based biosensor for the detection of ion channels in HEK293 cells.

## 4. Conclusions

In summary, we take advantages of the Exo III amplification strategy and molecular machines' amplification technique to create a photocleavable and entropy-driven based signal-amplifying biosensor, and demonstrate its utilization for ultrasensitive detection of ion channels in single-cell level. Effective monitoring of the cell ion channels (KV11.1) level on the HEK293 cell surface proved that the design strategy gives a facile and powerful protocol for analysis of the ion channels. This biosensor employed a photocleavable linker molecule, which smartly converted the ion channels' concentration to the DNA1 concentration via treated by irradiation. Under the contributing of Exo III amplification and entropy-driven molecular machines' amplification techniques, this biosensor produces an amplified signal to attain a highly sensitive detection of ion channels in HEK293 as low as a single-cell. Based on the advantages mentioned above, we have confidence in the biosensor that it holds great promise for ion channels or other proteins (via antibody-antigen reaction or aptamer-target reaction) in single-cell analysis. This is a new concept for single-cell research, and opens an opportunity for new biosensors fabrication which based on photocleavable reaction and amplification technique.

## CRediT authorship contribution statement

**Kai Zhang:** Conceptualization, Writing - review & editing, Supervision. **Wanting Huang:** Data curation, Software, Validation. **Hao Li:** Data curation, Software, Validation. **Minhao Xie:** Visualization. **Jiaying Wang:** Supervision, Conceptualization.

## Acknowledgment

This work was supported by the National Natural Science Foundation of China (21705061), the Jiangsu Provincial Key Medical Discipline (Laboratory) (ZDXKA2016017), General Program of Wuxi Health and Family Planning Commission (No. MS201738) and the Innovation Capacity Development Plan of Jiangsu Province (BM2018023).

## Supplementary data

Supplementary data can be found in the online version.

## Declaration of interests

The authors declare that they have no known competing financial interests or personal relationships that could have appeared to influence the work reported in this paper.

## Appendix A. Supporting information

Supplementary data associated with this article can be found in the online version at doi:10.1016/j.bios.2019.02.065.

## References

Abbas, H.A., Pant, V., Lozano, G., 2011. The ups and downs of p53 regulation in hematopoietic stem cells. Cell Cycle 10 (19), 3257–3262.
Agasti, S.S., Liong, M., Peterson, V.M., Lee, H., Weissleder, R., 2012. Photocleavable DNA barcode–antibody conjugates allow sensitive and multiplexed protein analysis in

single cells. J. Am. Chem. Soc. 134 (45), 18499–18502.
Altelaar, A.F.M., Heck, A.J.R., 2012. Trends in ultrasensitive proteomics. Curr. Opin. Chem. Biol. 16 (1–2), 206–213.
Bhuniya, S., Maiti, S., Kim, E.-J., Lee, H., Sessler, J.L., Hong, K.S., Kim, J.S., 2014. An activatable theranostic for targeted cancer therapy and imaging. Angew. Chem. Int. Ed. 53 (17), 4469–4474.
Cui, L., Ke, G., Zhang, W.Y., Yang, C.J., 2011. A universal platform for sensitive and selective colorimetric DNA detection based on exo III assisted signal amplification. Biosens. Bioelectron. 26 (5), 2796–2800.
Elsholz, B., Nitsche, A., Achenbach, J., Ellerbrok, H., Blohm, L., Albers, J., Pauli, G., Hintsche, R., Worl, R., 2009. Electrical microarrays for highly sensitive detection of multiplex PCR products from biological agents. Biosens. Bioelectron. 24 (6), 1737–1743.
Fu, J., Yu, C., Li, L., Yao, S.Q., 2015. Intracellular delivery of functional proteins and native drugs by cell-penetrating poly(disulfide)s. J. Am. Chem. Soc. 137 (37), 12153–12160.
Issadore, D., Chung, J., Shao, H., Liong, M., Ghazani, A.A., Castro, C.M., Weissleder, R., Lee, H., 2012. Ultrasensitive clinical enumeration of rare cells ex vivo using a micro-hall detector. Sci. Transl. Med. 4 (141) (141ra192-141ra192).
Kang, Y., Guo, J., Yang, T., Li, W., Zhang, S., 2015. Regulation of the human ether-a-go-go-related gene (hERG) potassium channel by Nedd4 family interacting proteins (Ndfips). Biochem. J. 472 (1), 71–82.
Li, C., Li, X., Wei, L., Liu, M., Chen, Y., Li, G., 2015. Simple electrochemical sensing of attomolar proteins using fabricated complexes with enhanced surface binding avidity. Chem. Sci. 6 (7), 4311–4317.
Lin, M., Song, P., Zhou, G., Zuo, X., Aldalbahi, A., Lou, X., Shi, J., Fan, C., 2016. Electrochemical detection of nucleic acids, proteins, small molecules and cells using a DNA-nanostructure-based universal biosensing platform. Nat. Protoc. 11, 1244.
Liu, J., Cui, M., Niu, L., Zhou, H., Zhang, S., 2016a. Enhanced peroxidase-Like properties of graphene–hemin-composite decorated with Au nanoflowers as electrochemical aptamer biosensor for the detection of K562 leukemia cancer cells. Chem. Eur. J. 22 (50), 18001–18008.
Liu, J., Cui, M., Zhou, H., Yang, W., 2017. DNAzyme based nanomachine for in situ detection of microrna in living cells. ACS Sens. 2 (12), 1847–1853.
Liu, J., Cui, M., Zhou, H., Zhang, S., 2016b. Efficient double-quenching of electrochemiluminescence from CdS:Eu QDs by hemin-graphene-Au nanorods ternary composite for ultrasensitive immunoassay. Sci. Rep. 6, 30577.
Liu, J., Xin, X., Zhou, H., Zhang, S., 2015. A ternary composite based on graphene, hemin, and gold nanorods with high catalytic activity for the detection of cell-surface glycan expression. Chem. Eur. J. 21 (5), 1908–1914.
Liu, J., Zhou, H., Xu, J.-J., Chen, H.-Y., 2012. Switchable 'on–off–on' electrochemical technique for direct detection of survivin mRNA in living cells. Analyst 137 (17), 3940–3945.
Qian, Z., Xu, X., Amacher, J.F., Madden, D.R., Cormet-Boyaka, E., Pei, D., 2015. Intracellular delivery of peptidyl ligands by reversible cyclization: discovery of a PDZ domain inhibitor that rescues CFTR activity. Angew. Chem. Int. Ed. 54 (20), 5874–5878.
Sato, S.-i., Watanabe, M., Katsuda, Y., Murata, A., Wang, D.O., Uesugi, M., 2015. Live-cell imaging of endogenous mRNAs with a small molecule. Angew. Chem. Int. Ed. 54 (6), 1855–1858.
Shackleton, M., Quintana, E., Fearon, E.R., Morrison, S.J., 2009. Heterogeneity in cancer: cancer stem cells versus clonal evolution. Cell 138 (5), 822–829.
Steel, A.B., Herne, T.M., Tarlov, M.J., 1998. Electrochemical quantitation of DNA immobilized on gold. Anal. Chem. 70 (22), 4670–4677.
Tay, S., Hughey, J.J., Lee, T.K., Lipniacki, T., Quake, S.R., Covert, M.W., 2010. Single-cell NF-[kgr]B dynamics reveal digital activation and analogue information processing. Nature 466 (7303), 267–271.
Wang, B., Liu, Z., Ma, Z., Li, M., Du, L., 2016. Astemizole derivatives as fluorescent probes for hERG potassium channel imaging. ACS Med. Chem. Lett. 7 (3), 245–249.
Wu, L., Qu, X., 2015. Cancer biomarker detection: recent achievements and challenges. Chem. Soc. Rev. 44 (10), 2963–2997.
Wu, M., Singh, A.K., 2012. Single-cell protein analysis. Curr. Opin. Biotechnol. 23 (1), 83–88.
Yang, G.-Y., Li, C., Fischer, M., Cairo, C.W., Feng, Y., Withers, S.G., 2015. A FRET probe for cell-based imaging of ganglioside-processing enzyme activity and high-throughput screening. Angew. Chem. Int. Ed. 54 (18), 5389–5393.
Yang, H., Gao, Y., Wang, S., Qin, Y., Xu, L., Jin, D., Yang, F., Zhang, G.-J., 2016. In situ hybridization chain reaction mediated ultrasensitive enzyme-free and conjugation-free electrochemcial genosensor for BRCA-1 gene in complex matrices. Biosens. Bioelectron. 80, 450–455.
Yang, X.-J., Zhang, K., Xu, J.-J., Chen, H.-Y., 2018. In situ visualization of hERG potassium channel via dual signal amplification. Anal. Chem. 90 (10), 6199–6205.
Yao, B., Liu, Y., Tabata, M., Zhu, H., Miyahara, Y., 2014. Sensitive detection of microRNA by chronocoulometry and rolling circle amplification on a gold electrode. Chem. Commun. 50 (68), 9704–9706.
Yu, T., Wei, Q., 2018. Plasmonic molecular assays: recent advances and applications for mobile health. Nano Res. 11 (10), 5439–5473.
Yuan, Y., Zhang, C.-J., Gao, M., Zhang, R., Tang, B.Z., Liu, B., 2015. Specific light-up bioprobe with aggregation-induced emission and activatable photoactivity for the targeted and image-guided photodynamic ablation of cancer cells. Angew. Chem. Int. Ed. 54 (6), 1780–1786.
Zhou, G., Zhang, X., Ji, X., He, Z., 2013. Ultrasensitive detection of small molecule-protein interaction via terminal protection of small molecule linked DNA and Exo III-aided DNA recycling amplification. Chem. Commun. 49 (78), 8854–8856.
Zhou, H., Liu, J., Xu, J.-J., Zhang, S.-S., Chen, H.-Y., 2018. Optical nano-biosensing interface via nucleic acid amplification strategy: construction and application. Chem. Soc. Rev. 47 (6), 1996–2019.
Zhu, J., Gan, H., Wu, J., Ju, H., 2018. Molecular machine powered surface programmatic chain reaction for highly sensitive electrochemical detection of protein. Anal. Chem. 90 (8), 5503–5508.